TISSUE ENGINEERING: Part C
Volume 24, Number 6, 2018

DOI: 10.1089/ten.tec.2018.0040

termis
Tissue Engineering
& Regenerative Medicine
International Society

METHODS ARTICLE

The Development of Newborn Porcine Models for Evaluation of Tissue-Engineered Small Intestine

Mitchell R. Ladd, MD, PhD,[1,*] Laura Y. Martin, MD,[1,*] Adam Werts, DVM, PhD,[1] Cait Costello, PhD,[2] Chhinder P. Sodhi, PhD,[1] William B. Fulton, MS,[1] John C. March, PhD,[2] and David J. Hackam, MD, PhD[1]

Short bowel syndrome (SBS) is a major cause of morbidity and mortality in the pediatric population, for which treatment options are limited. To develop novel approaches for the treatment of SBS, we now focus on the development of a tissue-engineered intestine (also known as an ''artificial intestine''), in which intestinal stem cells are cultured onto an absorbable bioscaffold, followed by implantation into the host. To enhance the translational potential of these preclinical studies, we have developed three clinically relevant models in neonatal piglets, which approximate the size of the human infant and were evaluated after implantation and establishment of intestinal continuity over the long term. The models included (1) a staged, multioperation approach; (2) a single operation with a de-functionalized loop of small intestine; and (3) a single operation with an intestinal bypass. The first model had complications related to multiple operations in a short time period, including surgical site infections and wound hernias. The second model avoided wound complications, but was associated with high ostomy output, local skin breakdown, and systemic dehydration with associated electrolyte imbalances. The third model was the most effective, although resulted in stoma prolapse. In summary, we have now developed and evaluated three operative methods for the long-term evaluation of the artificial intestine in the piglet, and conclude that a single operation with a de-functionalized loop of small intestine may be an optimal approach for evaluation over the long term.

Keywords: tissue-engineered small intestine, porcine model, newborn porcine models

Introduction

Short bowel syndrome (SBS) is a devastating condition in which the absorptive surface of the intestinal mucosa is insufficient to meet the nutritional needs of the patient, resulting in inadequate growth and development.[1–4] In children, the leading causes of SBS include necrotizing enterocolitis (an inflammatory condition that leads to inflammation and necrosis of large amounts of the small intestine), congenital intestinal atresia, intestinal volvulus, and gastroschisis.[1–4] SBS remains a significant cause of morbidity and mortality in the pediatric population in which the estimated 5-year mortality approaches 40%,[2,3,5,6] with most deaths occurring from sepsis and liver failure. Current therapy for SBS aims to restore enteral autonomy, by medical, dietary, or surgical intervention.[2,3,5,7] Unfortunately, these therapies are ineffective for many patients, ultimately requiring an intestinal transplant with its numerous associated complications.[2,6,7]

The development of a tissue-engineered small intestine (also known as an artificial intestine) has emerged as a potential investigative option for the treatment of children with SBS.[8–15] The requirements for the successful development of a functional intestinal graft in the laboratory include the following: (1) a source of progenitor cells with the capacity to grow and differentiate into a well-differentiated absorptive intestinal mucosal surface, (2) a scaffold capable of supporting cellular growth, (3) adequate vascularization of the newly engineered tissue, and (4) an intact neural network to promote peristalsis.[9–17] Most investigators have utilized rodent models to evaluate the potential efficacy of each of these components, and while such studies have yielded some very useful proof-of-concept data, they have been limited by the physical and structural differences between rodents and humans. While there have been reports of successful placement of tissue-engineered small intestinal constructs in large animals, most prior studies have been limited by replacing only a small

[1]Division of Pediatric Surgery, Department of Surgery, Johns Hopkins University School of Medicine, Baltimore, Maryland.
[2]Department of Biomedical Engineering, Cornell University, Ithaca, New York.
*These two authors contributed equally to this work.

portion of the intestinal circumference.[12,18,19] We therefore now sought to develop a large animal model for the long-term placement and evaluation of a tissue-engineered small intestinal graft using the neonatal piglet, which shares structural and physiological properties with the newborn human infant. Specifically, we designed three different surgical approaches and evaluated clinically relevant outcomes of each, to define the optimal operative technique for testing the artificial gut, and ultimately its use in humans.

Materials, Methods, and Model Design

Scaffold synthesis

Scaffolds were synthesized from either poly(ethylene-co-vinyl acetate) (PEVA; Sigma-Aldrich, 340502) or poly(glycerol sebacate) (PGS; Sigma-Aldrich, 900210) into structures with a three-dimensional crypt-villus architecture that bears remarkable similarity to the native intestine as we have previously reported.[20–22] In brief, laser ablation (Versalaser; Universal Laser Systems, Scottsdale, AZ) was used to create a template array of 500 μm deep, high aspect ratio holes on a polymethylmethacrylate (PMMA) template. Polydimethylsiloxane (PDMS; Dow Corning, MI) was used to fabricate $\sim 8\,\text{cm} \times 4\,\text{cm}$ replicas of the final bioscaffold with a full villus array as described previously.[23] Molten agarose (3% in water; Sigma, St Louis, MO) was then poured over the PDMS scaffolds and cooled at room temperature to form hydrogel replicas of the initial PMMA molds. Scaffolds were then fabricated using a modified version of a porogen leaching/thermally induced phase separation technique.[21] The polymer solution was then poured into the mold and processed according to previously published methods to create the final porous scaffold.[21] For PEVA scaffolds, a 10% PEVA solution in chloroform was used and for PGS scaffolds, either a 20% or 30% PGS solution in chloroform was used. For both polymers, just before pouring in the mold, the solutions were mixed with preminced sodium bicarbonate powder (400 mg/mL) as the porogen. For PGS scaffolds, either a 2% or 4% 4,4′-methylenebis(phenyl isocyanate) (MDI; Sigma-Aldrich, 256439) crosslinker was dissolved before adding the porogen to optimize their stiffness and degradation.

Surgical techniques for implantation of the tissue-engineered intestinal constructs

All experiments were approved by the Johns Hopkins University Animal Care and Use Committee (Protocol numbers SW15M208 and SW16M440). Experiments were performed on piglets (at the ages described below), which were obtained from Archer Farms (Darlington, MD). Piglets were housed in single or paired enclosures before and/or after surgery. All surgeries were performed under isoflurane anesthesia using a Narkomed system (North American Drager, Houston, TX). Twenty-four hours prior to surgery, piglets were given a liquid only diet, a weight-based pediatric Miralax bowel preparation, and were made Nil Per Os at least 8 hours before an operation. Preoperatively and postoperatively, animals were fed enterally with milk or Ensure (depending on age of the animal) and transitioned to solid food when appropriate. Additional supplementation of electrolyte solution, fiber, and protein supplements is further detailed in the ''Materials, Methods, and Model Design'' section. Euthanasia was performed with Euthasol (100 mg/kg) after sedation with ketamine/xylazine (20 mg/kg and 2 mg/kg, respectively) at the completion of experiment, or sooner if there were signs of distress.

The following experimental surgical models detailed below were developed to evaluate the performance of a composite graft of synthetic scaffold seeded with progenitor cells after implantation into piglets.

Model 1: omental implantation model. The omental implantation model subjected piglets to three sequential procedures: the harvest of stem cells, omental implantation of constructs, and connection of construct to the intestine with an omental pedicle ($n = 5$, Fig. 1). Four-day-old piglets underwent laparotomy for isolation of stem cells from the distal small bowel. A longitudinal full thickness midline skin incision was made, and a 3 cm segment of distal ileum, 20 cm upstream from the ileocecal valve, was resected. The intestine was then primarily reanastomosed in an end-to-end manner with vicryl sutures. The midline incision was closed in layers with PDS, vicryl, and biosyn skin closure. Intestinal crypts were then isolated from the resected intestine (using the first cell isolation technique described below), expanded in culture, and seeded onto PEVA scaffolds *in vitro* for 5 days. At 9 days of age, a second laparotomy was performed to implant the grafts in the omentum. After laparotomy, the omentum was freed from its attachments to the spleen to create a flap in which the graft was implanted. Vascularization of the implant was assessed at multiple time points in different animals. At 6 weeks, one piglet achieved placement of the graft into continuity with native intestine. To place the graft in continuity, a third laparotomy was performed, the graft was mobilized *en bloc* with its vascularizing omentum, and then anastomosed in an end-to-end manner with native ileum using vicryl suture. The surgeries and outcomes for Model 1 are summarized in Table 1.

Model 2: single surgery construct implantation in continuity with intestinal diversion. The second surgical model had the goal of placing constructs in continuity with the small intestine using a single operation (Figs. 2 and 3). The graft and anastomoses were then protected from the fecal stream by performing a proximal ileostomy ($n = 5$). In addition, we attempted to create a distal mucus fistula for possible serial endoscopic interrogation of the graft while piglets were still living. Moreover, we foresaw that if the animals survived to the point of testing absorptive function, the proximal ostomy could be reversed, therefore routing the fecal stream through the construct, while the remaining distal ostomy would still allow for ongoing endoscopic interrogation of the implanted graft. In animals receiving cell-seeded scaffolds, stem cell isolation was performed during the operation (using the second cell isolation techniques described below), after which they were seeded onto a scaffold intraoperatively before being directly anastomosed with native intestine. Two slightly varying surgical methods were employed in model 2.

*Double-loop ostomy (*n = *4) method (Fig. 2).* Surgery was performed through a single longitudinal midline incision. Grafts were placed in direct continuity with a diverted loop of intestine that was isolated by creating a proximal double-barrel diverting loop stoma for fecal diversion and a distal

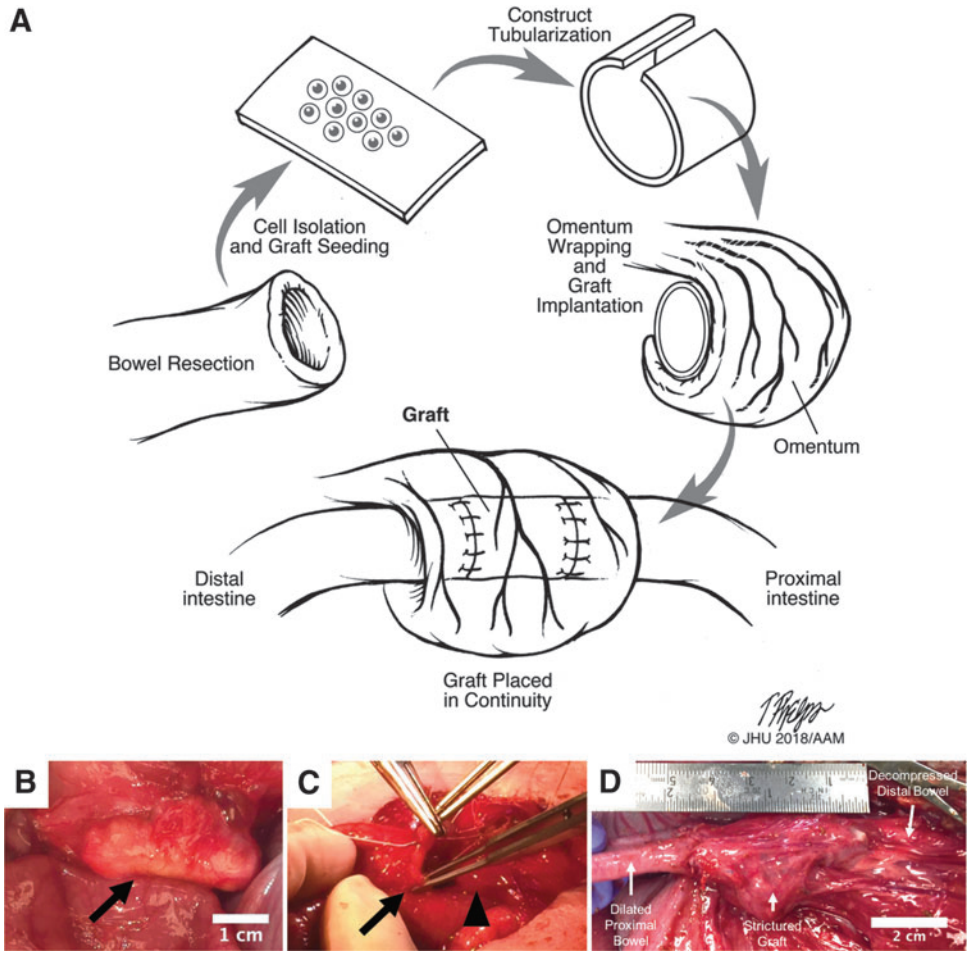

FIG. 1. **(A)** Schematic of the operative stages for pig model 1. **(B)** Scaffold construct implanted in the omentum (indicated by *arrow*). **(C)** The scaffold was anastomosed to the small bowel on both ends, putting it into continuity with the intestinal stream (*arrow* indicates small bowel lumen being sewn to one end of the scaffold indicated by the *arrowhead*). **(D)** At euthanasia, 5 days after placement in continuity, the scaffold had strictured and was no longer patent. The proximal bowel was significantly dilated with downstream decompression of the bowel.

double-barrel mucous fistula for drainage of distal mucous secretions. The distal double-barrel ostomy also served as an access point for attempts at evaluation of the grafts. Three animals were placed into the intestinal reanastomosis-only control group to test the surgical model without placement of scaffold. After incision, a 20 cm segment of bowel was identified 40 cm proximal to the ileocecal valve. Sites for diverting stoma and mucous fistula were identified and brought through the skin, but not opened or matured. A 3 cm segment of ileum from within the diverted loop was then resected. For the reanastomosis-only control group, an end-to-end anastomosis of the native ileum was performed. The omentum was then mobilized away from the spleen to wrap around the anastomoses. The abdomen was closed in layers. Then, the stoma and mucous fistula were opened and matured. In this model, a fourth animal underwent placement of scaffold (20% PGS, 2% MDI, unseeded). In this animal, the above surgery was performed, except that after resection of the 3 cm ileal segment from the diverted loop, the scaffold was anastomosed in an end-to-end manner proximally and distally with the native ileum. Finally, omentum was mobilized to envelope the scaffold and anastomoses. The details of the operations performed for this group are in Table 2.

Of note, after operating on the first animal in the method described in model 2, it was clear that the animals would have high ostomy output (4–5 L per day) requiring aggressive fluid replacement. Thus, for the remaining animals in this cohort, we placed left external jugular tunneled broviac catheters for maintaining intravenous access, and fluid and medicine administration.

End ileostomy with distal mucous fistula method (Fig. 3, n = 1). A single animal underwent this method at 6 weeks of age. This animal had a scaffold (20% PGS, 4% MDI, unseeded) placed in intestinal continuity downstream of a mucous fistula. The surgery was performed similarly to the double-loop ostomy method with the following two differences. First, a transverse laparotomy was made. Second, the proximal diverting stoma and distal mucous fistula were performed as end stomas (as opposed to two double-barrel ostomies) with no intervening bowel between the two (Fig. 3). The enterotomy was performed 40 cm upstream from the ileocecal valve. At a point 5 cm distal to the mucous fistula, a 3 cm segment of bowel was resected and then the construct was placed in an end-to-end manner, such that it was 5 cm distal to the mucous fistula. Omentum was mobilized to envelope the construct.

Model 3: single surgery construct implantation in continuity with intestinal bypass (Thiry-Vella loop). In this surgical model ($n = 6$), which is a modified form of the Thiry-Vella loop, a de-functionalized intestinal loop was brought to the skin with two mucous fistulas to drain the secretions of the loop and then bypassed by the remainder of the bowel[24–30] (Fig. 4). In this manner, the loop was entirely excluded from

Table 1. The First Model Involving Removal of Intestinal Tissue, Implantation into the Omentum, and Finally Anastomosis in Continuity with the Small Bowel

Animal	*Gender*	*Surgeries*	*Age at surgeries (days)*	*Age at euthanasia (days)*	*Euthanasia reason*	*Weights (kg)*	*Complications*	*Construct outcome*
1 (228)	Female	(1) 10 cm SBR	4			1.4	(1) Wound infection	
		(2) 5-Day organoid seeded PEVA scaffold in omentum	9			1.9	(2) Wound dehiscence and hernia postoperatively	
		(3) Exploration, no scaffold found, euthanasia	54	54	No construct for anastomosis	9.4		Not present
2 (226)	Female	(1) 10 cm SBR	4			1.46		
		(2) 5-Day organoid seeded PEVA scaffold in omentum	9			1.9	(2) Small bowel injury, SBR, and anastomosis during operation; wound dehiscence and hernia postoperatively	
		(3) Placed construct in continuity, rectopexy, hernia repair	44			6.1	Rectal prolapse occurred, age 39–44 days	
				49	Recurrent rectal prolapse			Stricture at construct anastomosis
3 (225)	Female	(1) 10 cm SBR	4			1.86		
		(2) 5-Day organoid seeded PEVA scaffold in omentum	9			2.4	(2) Wound dehiscence and hernia postoperatively	
		(3) Exploration, attempted anastomosis of construct to small bowel, but construct separated from fibrous capsule; euthanasia	37	37	Construct without ability to anastomose; prolonged anesthesia time	7.1		Construct separated from fibrous omental capsule
4 (227)	Female	(1) 10 cm SBR	4			1.24		
		(2) 5-Day organoid seeded PEVA scaffold in omentum	9			1.9	(2) Scaffold had bacterial colonization on implantation; wound infection, wound dehiscence, hernia	
		Euthanasia		29	Found down; hypoglycemic	3.0		Construct explanted from omentum
5 (229)	Female	(1) Unseeded scaffold implantation into omentum	4			1.6		
		(2) Exploration of scaffold	22			4.5		Scaffold not well incorporated/ encapsulated at this time
		(3) Reexploration of scaffold, euthanasia	54	54	Decision to change scaffold material due to poor incorporation of PEVA scaffolds	12.4		Vascular imaging with cardiogreen, explantation of scaffold

The scaffolds used in these animals were made of PEVA.
SBR, small bowel resection; PEVA, poly(ethylene-co-vinyl acetate).

continuity with the intestine and was not exposed to the fecal stream. Two pigs underwent placement of scaffold consisting of 20% PGS, 4% MDI ($n=1$) or 30% PGS, 4% MDI ($n=1$) without seeded cells. Four pigs underwent placement of seeded scaffolds (grafts) with 30% PGS, 4% MDI. Following transverse laparotomy incision, the ileocecal valve was identified. A 20 cm segment of intestine was identified and isolated, with distal transection 25 cm proximal to ileocecal valve and proximal transection 45 cm proximal to ileocecal valve. Intestinal continuity was restored with end-to-end anastomosis of the proximal and distal ileal ends, leaving the loop completely out of continuity with the native intestine. Two sites for mucous fistulas were then identified on the skin, and the ends of the de-

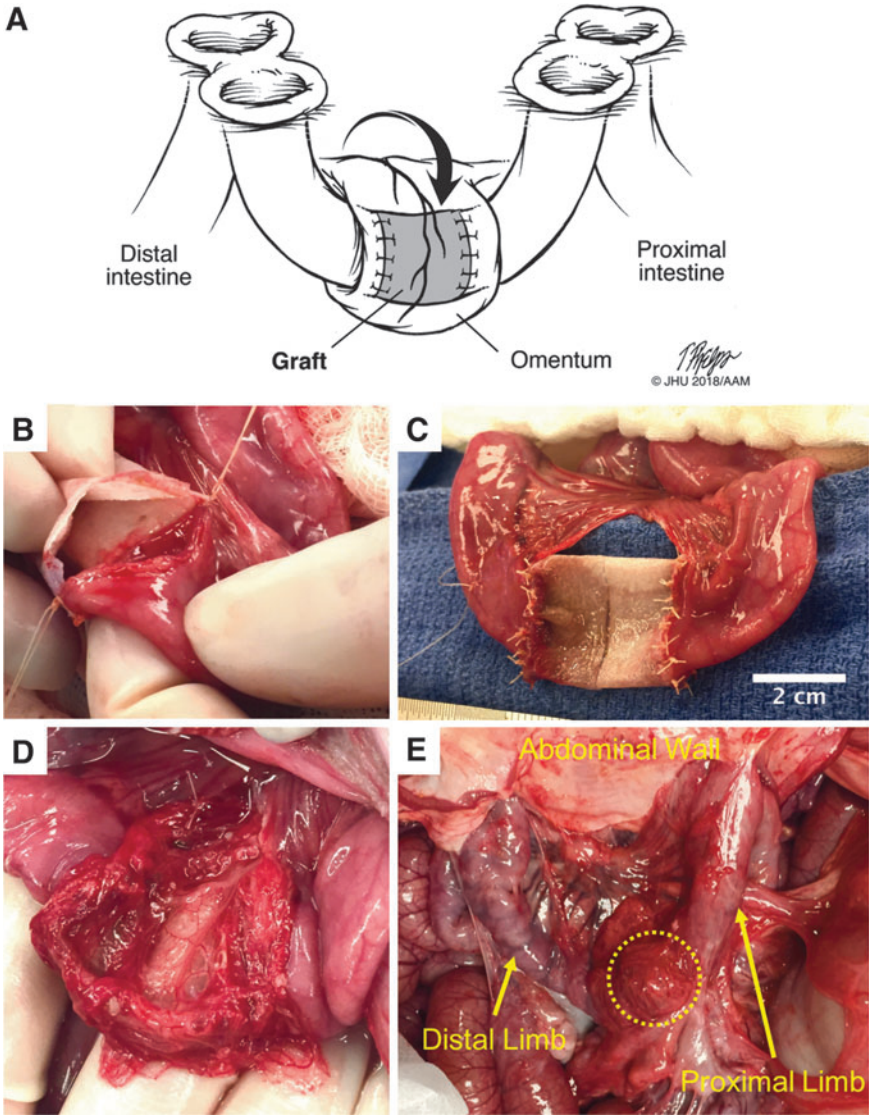

FIG. 2. **(A)** Illustration of surgical model 2 double-loop ostomy method with diverting double-barrel, loop ileostomy and double-barrel, loop mucous fistulas. **(B)** Intraoperative image of PGS graft being anastomosed to native intestine. **(C)** Completed anastomosis of graft to intestine. **(D)** The omentum has been mobilized and wrapped around the graft. **(E)** At euthanasia, 16 days after implantation, due to complications from high ostomy output, the graft can be seen (within *dotted* outline) still wrapped in omentum. The graft had completely strictured and some adjacent bowel had adhered to the inferior portion of the scaffold. The proximal and distal limbs of the isolated loop can be seen going up to the ostomy openings at the abdominal wall. PGS, poly(glycerol sebacate).

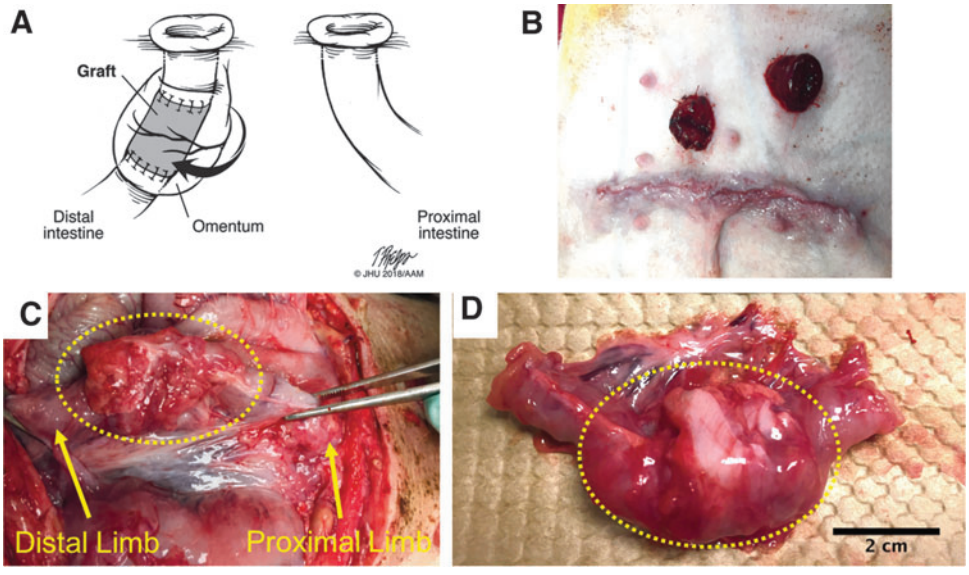

FIG. 3. **(A)** Illustration of surgical model 2 end ileostomy with distal mucous fistula method. **(B)** Abdominal wall at the completion of surgery demonstrating the end ileostomy and mucous fistula. **(C)** At 1 month, the graft (within *dotted* outline) demonstrated a dense fibrotic capsule and was not well incorporated with the intestine. The proximal limb proceeds to the abdominal wall where it forms the mucous fistula. **(D)** The graft (within *dotted* outline) explanted with attached small intestine.

Table 2. The Second and Third Animal Models in Which Only One Operation Was Performed

Animal	*Gender*	*Surgeries*	*Age at surgery (weeks)*	*Age at euth. (weeks)*	*Euth. reason*	*Weights (kg)*	*Construct type*	*Complications*	*Construct outcome*
6 (415)	Male	(1) Double-loop ostomy, 3 cm SBR from de-functionalized segment	5.9			9.05	None-Control	Skin irritation, SSI, high ostomy output, severe electrolyte abnormalities	
				7.1	Due to complications, concern for sepsis	7.16			Intact primary anastomosis
7 (413)	Male	(1) Double-loop ostomy, 3 cm SBR, interposition construct implant in de-functionalized segment without cells, reexploration, repair of scaffold	6.6			11.8	20% PGS, 2% MDI unseeded	Disruption of scaffold immediately postoperatively, which required repair	
		(2) Broviac placement	8.3			9.5			
		Euthanasia		8.9	Dumping syndrome, enteroenteral fistula, high ostomy output, electrolyte abnormalities	10			Strictured
8 (427)	Male	(1) Double loop ostomy, 3 cm SBR from de-functionalized segment, broviac placement	5.1			4.9	None, Control	High ostomy output, hypomagnesemia, respiratory stridor	
				5.9	Acute severe strangulated prolapse of proximal ostomy	4			Intact primary anastomosis
9 (414)	Female	(1) Double-loop ostomy, 3 cm SBR from de-functionalized segment, broviac placement	8.6			13.75	None, Control		
				9.1	Found dead, eviscerated	13.75		Unplanned death	N/A
10 (H57)	Female	(1) End ileostomy, distal mucous fistula, 3 cm SBR from bowel distal to mucous fistula with implantation of construct, broviac	6			9.99	20% PGS with 4% MDI unseeded	High output fistula, electrolyte disturbances	
				9.9	Time point reached	11.7			Dense fibrotic capsule, not well incorporated
11 (H58)	Female	(1) Bypass model with de-functionalized loop, 3 cm SBR with interposition construct implantation in de-functionalized segment, broviac	8			11.26	20% PGS with 4% MDI unseeded	Concern for bowel obstruction on POD3	
		(2) Exploratory laparotomy, decompression of intestine, pexy of small bowel proximal and distal to bypass segment, pexy of construct	8.4			11.61			Scaffold intact, anastomoses to scaffold intact, primary anastomosis of bypass segment intact and patent
				11.4	Time point reached	15			
12 (H174)	Female	(1) Bypass model with de-functionalized loop, 3 cm SBR with interposition construct implantation in de-functionalized segment, broviac, reinsertion broviac	8.1			12	30% PGS with 4% MDI unseeded	Broviac dislodged, had to be replaced during same operation; reducible prolapse of stomas 2–3 weeks postoperatively	
				14	Sepsis, necrotizing enteritis, severe thrombocytopenia, possibly all secondary to bacterial overgrowth of de-functionalized segment	19			Dense fibrotic capsule, collapsed scaffold, not well incorporated

(*continued*)

TABLE 2. (CONTINUED)

Animal	*Gender*	*Surgeries*	*Age at surgery (weeks)*	*Age at euth. (weeks)*	*Euth. reason*	*Weights (kg)*	*Construct type*	*Complications*	*Construct outcome*
13 (H173)	Female	(1) Bypass model with de-functionalized loop, 3 cm SBR with interposition construct implantation in de-functionalized segment	8.3			10.3	30% PGS with 4% MDI seeded	Reducible prolapse of stomas 2–3 weeks postoperatively	
				12.4	Found dead, cause of death undetermined, possible acute prolapse of ostomies and rectum	16			
14 (H267)	Female	(1) Bypass model with de-functionalized loop, 3 cm SBR with interposition construct implantation in de-functionalized segment	9.6			13.32	30% PGS with 4% MDI seeded	Reducible prolapse of stomas 2–3 weeks postoperatively	
				14	Time point reached	18			Dense fibrotic capsule, construct collapsed and not patent, not well incorporated
15 (H266)	Female	(1) Bypass model with de-functionalized loop, 3 cm SBR with interposition construct implantation in de-functionalized segment	9.1			—	30% PGS with 4% MDI seeded	Reducible prolapse of stomas 2–3 weeks postoperatively	
				13.3	Time point reached	18.4			Dense fibrotic capsule, construct had migrated intraluminally (fibrotic capsule maintained continuity with bowel), not well incorporated and construct was mobile inside lumen of bowel
16 (H265)	Female	(1) Bypass model with de-functionalized loop, 3 cm SBR with interposition construct implantation in de-functionalized segment	8.3			12.5	30% PGS with 4% MDI seeded	Reducible prolapse of stomas 2–3 weeks postoperatively	
				11.6	Time point reached	15			Dense fibrotic capsule, capsule partially collapsed, but patent, not well incorporated and easily separates from underlying capsule

Refer to article for more details, but in short, grafts were anastomosed to small bowel after a small bowel resection. The scaffolds were either seeded or unseeded with cells obtained during same operation and then wrapped in omentum while in continuity. In all cases, the fecal stream was diverted from the graft anastomosis using an evolving set of methods.

SBR, small bowel resection; PGS, poly(glycerol sebacate); MDI, 4,4′-methylenebis(phenyl isocyanate); POD, postoperative day; SSI, surgical site infection; NA, not applicable.

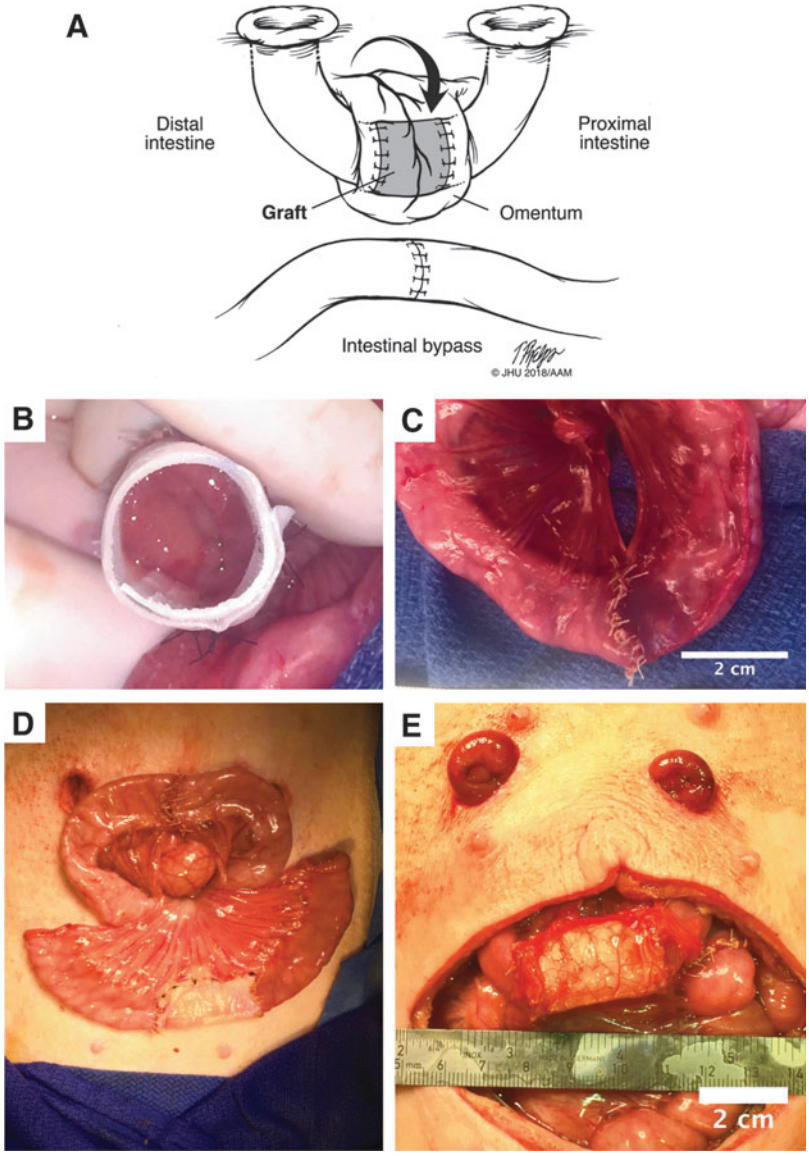

FIG. 4. **(A)** Illustration of surgical model 3, the Thiry-Vella loop. **(B)** Graft being anastomosed to native intestine. **(C)** Primary anastomosis of the bypass segment of intestine. **(D)** Both the bypass and graft implantation completed, but before stoma maturation. **(E)** The ostomies were brought through the abdominal wall. The omentum was wrapped around the graft.

functionalized loop were brought through the fascial openings. A 3 cm segment of bowel was then removed from within the de-functionalized loop. In those animals receiving no scaffold, the bowel was primarily reanastomosed. In animals receiving the scaffold alone, the scaffold was anastomosed in an end-to-end manner with native intestine of the de-functionalized loop. In animals receiving cell-seeded scaffolds (grafts), the resected 3 cm segment of ileum was used to isolate stem cells as described in method 2 below. Following isolation, the cells were seeded on the matrigel-coated scaffold at 37°C for ~30 min. The graft was then anastomosed in an end-to-end manner proximally and distally with the native ileum of the isolated intestinal loop. For seeded scaffolds, any remaining cell solution at this point was carefully injected through an angiocatheter into the lumen of the scaffold. In all cases, the omentum was then mobilized to wrap the entire construct. All mesenteric defects were closed, and both mucous fistulas were tacked to the abdominal fascia. The laparotomies were closed in layers. Both mucous fistulas were then matured.

Laser angiography for evaluation of perfusion

One animal in surgical model 1 and one animal in model 3 underwent laser angiography using the Spy Elite Imaging System (Novdaq Technologies, Inc., Richmond, Canada; model LC3000) with indocyanine green (2.5 mg/mL; MilliporeSigma, 21980). This was performed at 7 weeks in surgical model 1, after which the animal was euthanized. In surgical model 3, the procedure was performed at 6 weeks.

Enteroid isolation and scaffold seeding

Scaffolds were sterilized by soaking in 70% ethanol at room temperature under ultraviolet light for 30 min. After sterilization, they were rinsed in a culture hood with sterile phosphate-buffered saline (PBS) five times for 20 min each. Following the rinses, the scaffolds were coated with a 1:10 dilution of matrigel (Corning, 356237) into PBS for 30–60 min at 37°C.

Cells for seeding were isolated using two different techniques depending on the surgical model. The first technique used for surgical model 1 isolated primary intestinal crypts

similar to the methods described by Sato and collagues,[31,32] and were performed using sterile technique in a cell culture hood. In brief, the resected segment of bowel had its luminal contents washed out using PBS with 0.5 μg/mL Amphotericin B (Gibco, 15290-026), 50 μg/mL gentamicin (Amresco, E737), and 1% Pen/Strep (Quality Biological, 120-095-721). The mesentery was removed from the intestinal tissue and then the intestine was minced and placed in a conical tube with digestion media consisting of Dulbecco's modified Eagle's medium (DMEM; Gibco, 11965-092) with 1% Pen/Strep and 4 mM ethylenediaminetetraaceticacid (Quality Biological, 351-027-721) for 30–45 min at 4°C on a rotator. After incubation in digestion media, the conical tube containing the minced intestine was placed on ice to allow the cellular material to settle. The supernatant was discarded and then PBS (plus 10% fetal bovine serum [FBS]; Corning, 35-011-CV) was added and the tissue was vigorously triturated. After trituration, the tissue was centrifuged at 200 *g* for 5 min. These steps were repeated (removal of supernatant, addition of washing PBS, trituration, and centrifugation) until the tissue separated into layers with a clear sandy, light-colored layer appearing at the top of the pellet. This layer was carefully pipetted off and placed on a 70-μm filter, which was on top of a 50-mL conical tube. The filter was rinsed with 2–3 mL of enteroid base media consisting of Advanced DMEM/F12 (Gibco, 12634-010), 20% embryonic stem cell FBS (heat inactivated at 56°C for 30 min; Hyclone, SH3007003E), 2 mM L-glutamine (Gibco, 25030-081), 50 μg/mL gentamicin, 0.5 μg/mL Amphotericin B, 50 mM HEPES (Quality Biological, 118-089-721), 1 mM *N*-acetylcysteine (Fisher Scientific, 50-131-8141), 1× N-2 supplement (Gibco, 17502-048), and 1× B27 supplement (Gibco, 12587-010). The filter was then wrapped in parafilm on top of the conical tube and it was centrifuged at 200 *g* for 5 min. The cell solution that passed through the filter was the desired crypt cell population.

The cells were washed in enteroid base media and spun down at 200 *g* for 5 min. Afterward, the cells were labeled using Vybrant CM-Dil (Vybrant, V22888) following the manufacturer's instructions and incubating at 37°C for 15–20 min. After staining, the cells were washed in enteroid base media by centrifuging at 200 *g* for 5 min and resuspending in enteroid base media thrice. After the final wash, the cells were resuspended in a sufficient volume of enteroid base media to completely cover the scaffold and the cells were allowed to attach for 3 h at 37°C in the cell culture incubator. After 3 h, the media were gently changed to enteroid growth media, which contained enteroid base media plus 50 ng/mL Wnt3A (Fisher Scientific, 1324-WN-10/CF), 50 ng/mL Noggin (Novus Biological, NBP2-35098), 100 ng/mL R-Spondin (Fisher Scientific, 3474RS050), and 100 ng/mL epidermal growth factor (EMD Millipore, 324831). For surgical model 1, the cells were cultured in the growth medium for four days before reimplantation.

For surgical models 2 and 3, a second cell isolation technique was used due to the need for rapid isolation and reimplantation during the same surgery. The second cell isolation technique was adapted from methods used by Sala *et al.*[12] In brief, the intestine was taken from the operating suite to the laboratory where isolation was performed with sterile instruments in a sterile cell culture hood. The lumen was thoroughly rinsed with Hanks' Balanced Salt Solution (HBSS; Sigma, H9394) until it was free of stool. Afterward, the mesentery was removed and the bowel was minced in a cell culture plate until the pieces were ~2 mm or less in size. The minced tissue was then rinsed 3–5 more times with HBSS in a conical tube with the tissue being allowed to settle between washes. After washing, the tissue was digested with 0.25 mg/mL Dispase (Gibco, 17105-041) and 800 U/mL type I collagenase (Worthington, LS004196) at 37°C for 30 min on a shaker. After 30 min, the digestion was halted by adding cold modified enteroid base media consisting of Advanced DMEM/F12, 2 mM Glutamax (Invitrogen, 35050-061), 10 mM HEPES, 1× N-2 supplement, 1× B27 supplement, and 1× Primocin (Invivogen, ant-pm-2). The tissue was then centrifuged at 400 *g* for 5 min and resuspended in a sufficient volume of modified enteroid base media to completely cover the scaffold for seeding. At this point, the cells were returned to the operating suite where they were applied to the scaffold for ~30 min before implantation of the construct.

Before implantation, all scaffolds were tubularized with nonabsorbable suture such that they were ~3–4 cm in length. The diameter of the scaffold was adjusted to match the caliber of the bowel to which it was being anastomosed.

Histology, immunohistochemistry, and confocal imaging

Seeded scaffolds were imaged by fixing in 4% paraformaldehyde (PFA; Electron Microscopy Sciences, 15710) for 1 h at room temperature with 0.1% Triton-x 100 for permeabilization. The scaffolds were then rinsed, blocked with 5% donkey serum for 1 h, and then incubated with primary antibody at a dilution of 1:250 at 4°C overnight. They were then washed and incubated with secondary antibody at a dilution of 1:1000 overnight at 4°C. Finally, the scaffolds were rinsed, counterstained with 4′,6-diamidino-2-phenylindole (DAPI; Biolegend, 422801), and imaged on the confocal microscope as whole specimens.

Explanted tissue was prepared by fixation in 4% PFA at 4°C overnight. Afterward, the tissue was either processed through serial ethanol and histoclear washes into paraffin by a tissue processor (ThermoScientific; Mircom STP 120) or equilibrated with 30% sucrose at 4°C overnight. For samples that went through the tissue processor, they were next embedded in paraffin for sectioning. Samples in sucrose were then removed and embedded either in O.C.T. compound (Fisher Healthcare; Tissue-Plus) with liquid nitrogen and kept at −20°C until cryosectioning or embedded in 3% agarose for vibratome sectioning.

Fifty to hundred micrometer sections were cut using a vibratome, whereas thinner sections (10–50 μm) were cut using a cryotome (ThermoScientific; Cryostar NX50) or microtome (Carl-Zeiss; SLEE Cut 6062). Sections made with cryotome or vibratome then underwent immunohistochemical staining by blocking with 5% donkey serum for 1 h, primary antibody incubation overnight at 4°C at a dilution of 1:250, secondary antibody staining at a dilution of 1:1000 overnight at 4°C, and staining with DAPI, and finally were coverslipped with gelvatol for imaging. Paraffin-embedded sections were first deparaffinized and then underwent antigen retrieval with citric acid. After antigen retrieval, the sections were stained with the same sequence as sections made with the cryotome or vibratome. All images were obtained using a Nikon Eclipse Ti microscope (Nikon, Melville, NY). Antibodies to the following antigens were used: Ki67 (Abcam, ab15580-100), sucrase-isomaltase (Santa Cruz, sc-27603), muc2 (Santa Cruz, sc-15334), E-Cadherin (R&D, AF748), proliferating cell nuclear antigen (Santa Cruz, sc-

56), PeCAM/CD31 (BD Biosciences, 550274), smooth muscle α-actin (Sigma, SAB2500963), Endothelin A receptor (Abcam, ab76259), Endothelin B receptor (Abcam, ab65972), vimentin (Santa Cruz, sc-7558), and BrdU (Novus, NB500-169). F-actin was stained with rhodamine phalloidin (Sigma, R415).

Electron microscopy

Specimens for scanning electron microscopy (LEO FE-SEM 153; Zeiss) were fixed in 5% glutaraldehyde in 3 mM $MgCl_2$ and 0.1 M sodium cacodylate buffer, pH 7.2, overnight at 4°C. Afterward, they were rinsed thrice for 15 min each in 3 mM $MgCl_2$ and 3% sucrose in 0.1 M sodium cacodylate buffer. Next, specimens were fixed in 1% osmium tetroxide in 3 mM $MgCl_2$ in 0.1 M sodium cacodylate buffer for 1 h on ice. After osmium tetroxide fixing, the specimens were rinsed twice in deionized water for 5 min each before undergoing dehydration in graded series of ethanol. The final three changes in the dehydration were a 1:1 ratio of 100% ethanol and hexamethyldisilazane. Finally, the samples were placed in a dessicator to dry. Once dry, the samples were mounted on stands with carbon tape and then sputter-coated with gold-palladium before imaging.

Results

Scaffold optimization

Pig enteroids were successfully isolated from the intestine and were able to be cultured *in vitro* (Fig. 5A, B). In addition, these cells were cryopreserved and thawed and maintained viability.

In surgical model 1, we evaluated the PEVA scaffolds. While nonabsorbable, the scaffolds had excellent handling properties, were durable, and showed good support of cellular growth *in vitro* (Fig. 5C, D). However, *in vivo*, we found that the tissue failed to integrate well with the scaffold (Fig. 6) and thus we limited our evaluation to five animals (Table 1). In addition, while there was some vascularization to the tissue (Figs. 7 and 8A), the majority of omental tissue was easily sheered from the material (Fig. 6B), suggesting that poor vascularization of the neointestine had occurred. Because of these findings, we decided to fabricate our scaffolds with a biodegradable polymer.

PGS was chosen because it has been used for other soft tissue engineering applications, it is an elastomer that is easy to manipulate surgically, and has been shown to have good biocompatibility *in vivo*.[33] PGS had good *in vitro* cellular integration as demonstrated with immunohistochemistry (IHC) (Fig. 5E, F). However, placement of scaffolds containing 20% PGS and 2% MDI crosslinker resulted in rapid degradation *in vivo* by gross examination and electron microscopy (Fig. 9). Subsequent experiments with higher concentrations of PGS (up to 30%) and MDI (up to 4%) resulted in slower degradation, but at the expense of some of the tissue integration, which was noted on gross examination (Fig. 6). Ultimately, we settled on a PGS concentration of 30% and MDI concentration of 4% for our final construct.

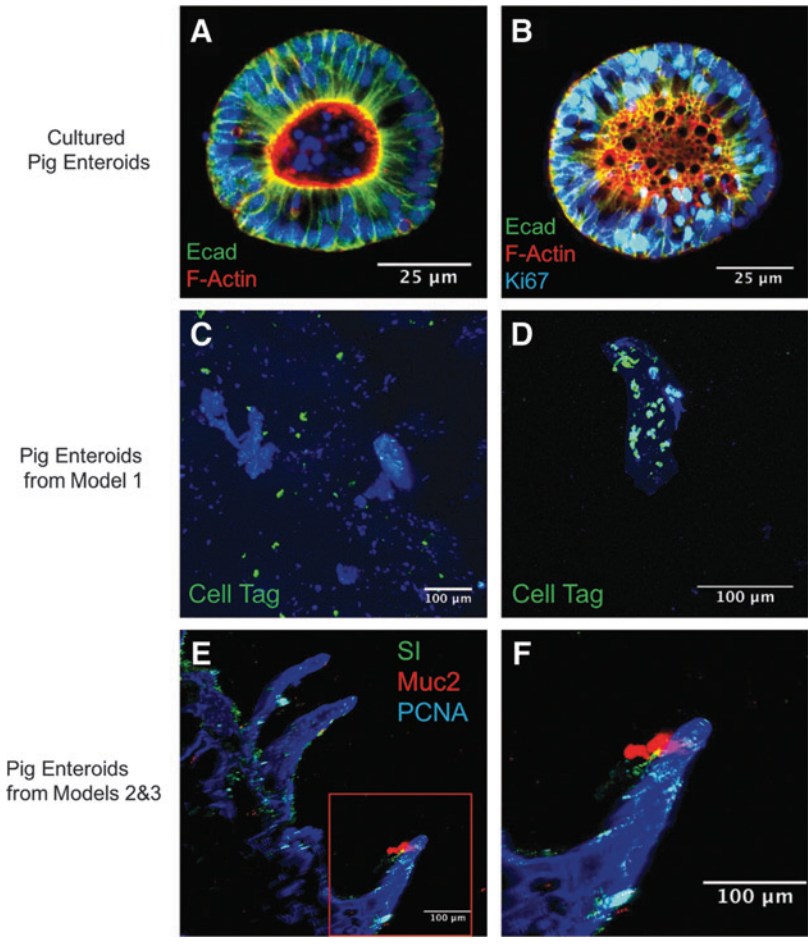

FIG. 5. **(A, B)** Intestinal stem cells could be successfully isolated from pig intestine (H266) and maintained in culture. **(C, D)** Intestinal stem cells from surgical model 1 on PEVA scaffolds after being labeled with a cell tag. **(E)** 200× magnification of cells isolated from surgical models 2 and 3 on PGS scaffolds. **(F)** Higher magnification view region highlighted in *red box* of image **(E)**. All images are counterstained with DAPI. PEVA, poly(ethylene-co-vinyl acetate; DAPI, 4′,6-diamidino-2-phenylindole.

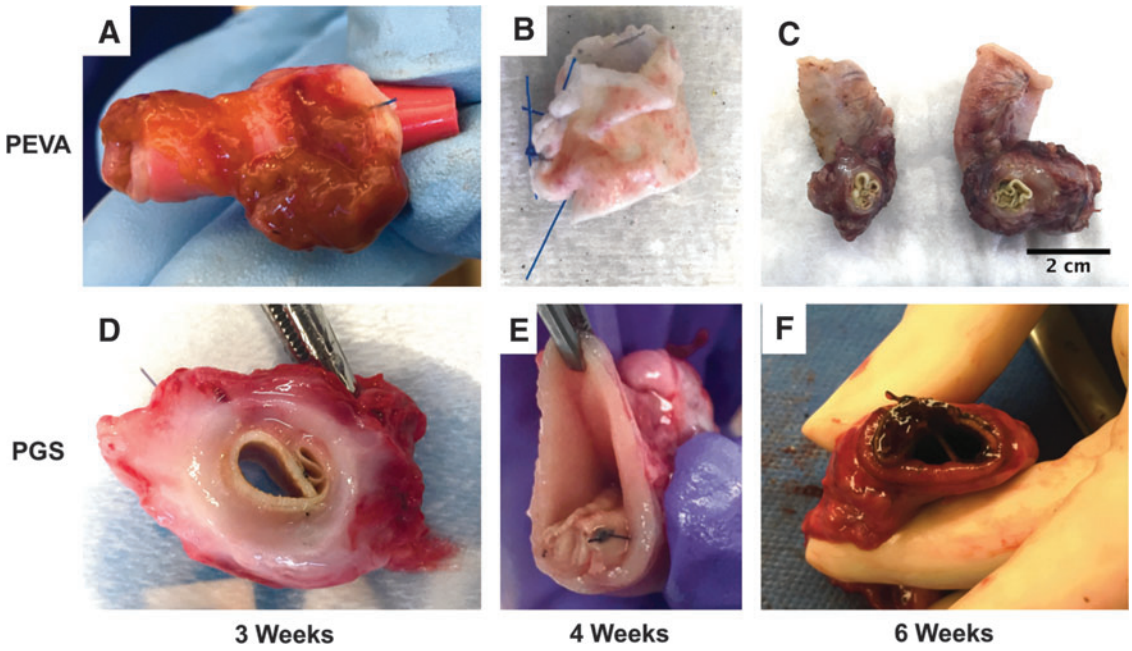

FIG. 6. Gross images of explanted grafts. **(A–C)** PEVA grafts. **(A)** Cell-seeded PEVA graft that was explanted from the omentum after 3 weeks. A *red* rubber catheter had been put in the lumen to try to prevent it from scarring down. Note the adherent omentum and supportive tissue. **(B)** Cell-seeded PEVA graft after explantation from the omentum at 4 weeks. This graft did not incorporate well and stripped from the surrounding tissue quite easily, leaving behind this somewhat bare graft seen here. **(C)** Cell-seeded PEVA graft from animal 226, which had been implanted in the omentum for 35 days before anastomosis in continuity with the small bowel. The graft remained in continuity for 5 days before euthanasia and then was explanted. The graft had significant stricture and inflammatory reaction. **(D–F)** PGS grafts performed better overall compared to PEVA grafts; however, the results were heterogeneous with some scaffolds having some degree of tissue integration and others that had almost none. **(D)** A seeded PGS graft shows improved integration over PEVA scaffolds after 3 weeks of implantation in surgical models 2 and 3. **(E)** Seeded PGS graft at 4 weeks with poor tissue integration. The scaffold has scarred into a tight cylinder with no lumen and was completely surrounded by native bowel lumen. **(F)** Unseeded PGS graft after implantation in surgical model 3 for 6 weeks demonstrated significant inflammation. It also had fibrosed down to a very narrow lumen. Clearly, while these particular scaffolds were good starting points for continuing our tissue-engineered small intestine work in large animals, the scaffolds will need further optimization before it will be successful in large animals.

Surgical outcomes

Model 1: omental implant model. In this model, we determined that the PEVA scaffold had the aforementioned shortcomings, although we were able to successfully place the artificial intestine into continuity with native bowel for several days (Fig. 8C). Ultimately, however, the construct scarred down and caused an obstruction, prompting euthanasia after 5 days of continuity (Fig. 6C). The individual outcomes of the omental implant model can be viewed in

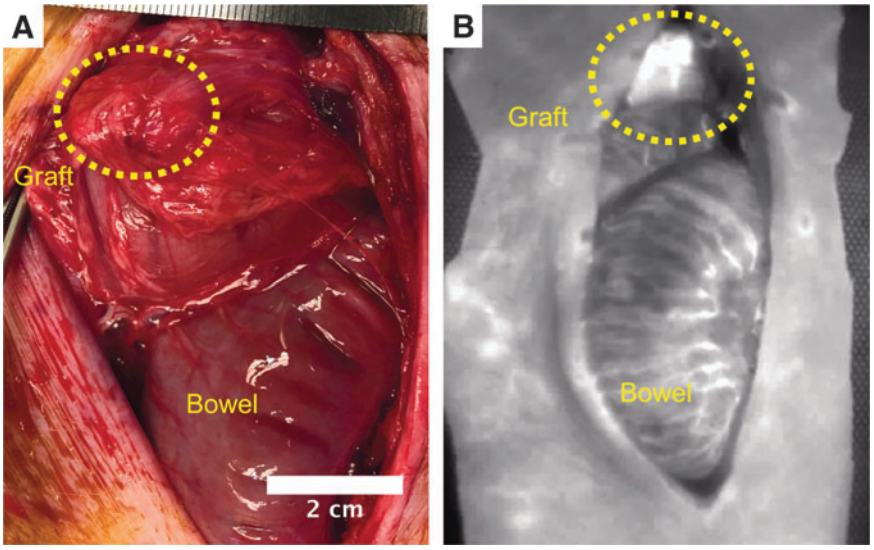

FIG. 7. **(A)** Graft demonstrated in the omentum of animal 229 (Table 1) at the time of euthanasia. **(B)** Laser angiography of the vasculature demonstrating a well-vascularized graft in the omentum after implantation for 7 weeks.

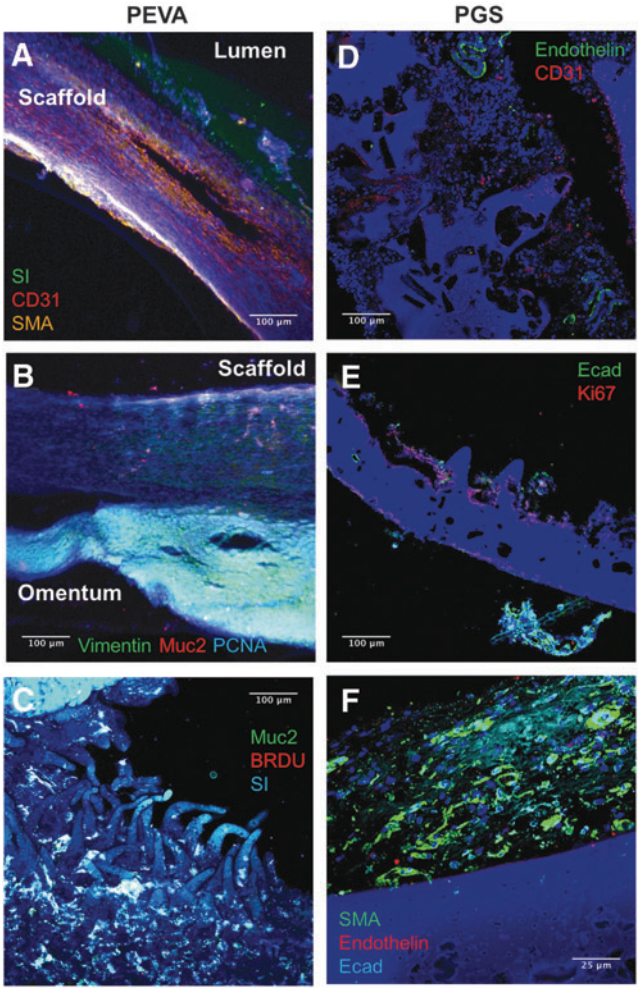

FIG. 8. Immunohistochemistry after explanation of the grafts. **(A)** Staining for SMA demonstrating possible myofibroblast growth in animal 227 three weeks after graft implantation. In addition, sucrase-isomaltase staining is observed on the mucosal or luminal side of the graft. CD31 demonstrates the beginning of neovascularization of the graft. **(B)** The graft from 227 demonstrating separation of the scaffold from surrounding tissue upon harvest. The graft demonstrates staining for myofibroblast marker vimentin, goblet cell marker Muc2, and proliferation marker PCNA. **(C)** Graft from 226, ~7 weeks after implantation, demonstrating positive staining for goblet cell marker Muc2, enterocyte marker SI, and for proliferation by BrdU. **(D)** Staining of a cell-seeded PGS graft from H173 4 weeks after implantation, demonstrating a small amount of neovascularization. **(E)** Cell-seeded graft from H267 demonstrating the scaffold architecture and a small amount of staining for the epithelial marker E-cadherin and proliferation marker Ki67 after implantation for 4 weeks. **(F)** Unseeded graft from H58 demonstrating the presence of myofibroblasts (SMA-positive cells) and the beginning of neovascularization in the presence of epithelial cells. All images are counterstained with DAPI. SI, sucrase-isomaltase; SMA, smooth muscle actin; Ecad, E-Cadherin; PCNA, proliferating cell nuclear antigen.

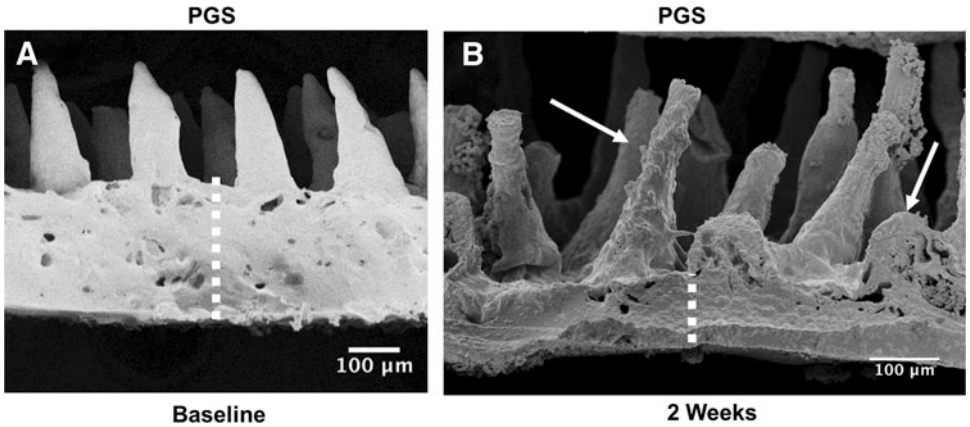

FIG. 9. **(A)** SEM of 20% PGS scaffold at baseline. The villus dimensions were ~100 μm wide at the base, 30–40 μm wide at the tip, and about 250–300 μm in height. **(B)** SEM of 20% PGS scaffold after implantation for 2 weeks (in animal 413) demonstrating scaffold degradation. Villus dimensions are roughly equal at 2 weeks, but the scaffold base has diminished (*dotted lines* indicating thickness of the base) and degradation is apparent (*arrows*). SEM, scanning electron microscopy.

Table 1. It is also noteworthy that we encountered surgical complications with the longitudinal incision and serial surgeries. Four of the five pigs developed hernias as they grew larger and the longitudinal incisions bore more weight. The incidence of wound infection was also high. As a result of these negative outcomes, we developed a new model to reduce the number of surgeries required and limit the need for reoperation through the same wound. In addition, due to increased inflammation and scarring noted with prolene suture closure, we transitioned to the use of PDS.

Model 2: single surgery construct implantation in continuity with intestinal diversion. In response to the high incidence of wound complications seen with serial surgeries, we sought to develop a single-staged surgical model and develop a method that could be translated most directly into human trials. In this model, the goal was to implant the scaffold directly into intestinal continuity and wrap it in omentum to develop supportive blood supply. To protect the graft from the fecal stream while this was occurring, the graft was placed downstream of a diverting ostomy. To more easily evaluate the scaffold without surgery at each stage, we also decided to create a distal mucous fistula such that the graft was isolated in an ileal loop (Fig. 2). In this model, we noted that rates of hernia and dehiscence were improved compared to use of longitudinal incisions. In addition, given the high intra-abdominal pressure encountered in the pigs, we found that attaching the stomas to the abdominal wall helped reduce the rate of stoma prolapse. However, this model had unforeseen consequences in pigs due to extremely high stoma output from the distal ileum. The output seen in pigs was significantly higher than that seen in humans with ileal stomas, along the order of 4–5 L per day. As a result, there were significant problems with electrolyte aberrations, dehydration, and skin breakdown. The same complications occurred with surgical model 2, end ileostomy with distal mucous fistula method. Ultimately, we were able to treat these complications successfully by daily administration of Ensure, 3 L of water repletion with glucose, sodium, and bicarbonate solution, as well as daily fiber, and imodium. Absorbent pads were placed on the abdomen at the site of the stomas and changed twice daily. These measures improved the electrolyte imbalances and skin breakdown. In this manner, we produced a model of diverting stoma that could be sustainable in pigs. However, given the time and resources necessary to sustain this model, we ultimately explored additional surgical options in the form of our final model. The outcomes of surgical model 2 can be seen in Table 2.

Model 3: single surgery construct implantation in continuity with intestinal bypass (Thiry-Vella loop). In this model, we completely isolated a bypassed loop containing the scaffold, with reanastomosis of native intestine proximal and distal to the loop. While we recognized internal hernia to be a potential complication, with careful tacking of the intestine and closure of the mesenteric defects, we did not have any internal hernias during the monitoring period of this study. In addition, due to ongoing complications with longitudinal incisions in the second model, including hernias and eviscerations in older and larger pigs, we altered our surgical technique to be performed through transverse incisions (this transition was made with surgical model 2, end ileostomy with distal mucous fistula method). Using this incision, we did not have any further hernias or eviscerations. The individual experimental conditions and outcomes of surgical model 3 can be viewed in Table 2. The results from this model were mixed, with some scaffolds incorporating well and others scarring with significant immune reaction (Fig. 6D–F). Also, some pigs showed evidence of cellular proliferation, vascularization, and epithelialization in IHC staining (Fig. 8D–F). However, on gross examination, the grafts did not incorporate well when placed directly in continuity with the intestine, with evidence of collapse and fibrosis (Fig. 6D–F). It should be noted that in three animals that had isolated ileal loops (one in model 2 and two in model 3), sepsis developed for unclear reasons, which we empirically attributed to bacterial overgrowth, mucosal atrophy, and bacterial translocation associated with the isolated loop and permeable graft. In an attempt to mitigate bacterial overgrowth and mucosal atrophy, we empirically began flushing the loop with glucose, but have not yet formally evaluated the effects that these interventions may have had on outcomes. In addition, as can be noted in Table 2, five out of the six animals in surgical model 3 developed reducible ostomy prolapses at both ostomy sites 2–3 weeks postoperatively, despite suturing the bowel proximal to the ostomy site to the abdominal wall. It should be noted that the initial intent of models 2 and 3 was to perform time points of 4, 6, and 8 weeks. However, due to the numerous complications that developed and the evolving approaches to address them, it was difficult to reach our longest time point. In addition, while we aimed to euthanize animals at 4 or 6 weeks, we occasionally made clinical judgments to euthanize an animal earlier to avoid an unexpected death or emergent euthanasia procedure. This resulted in the majority of animals surviving for 4–6 weeks after surgery with our longest time point of 7 weeks in animal 12 (H174).

Discussion

This article describes the development of an experimental model of SBS in the newborn piglet, and provides a translationally relevant platform for the study of an artificial intestine for the treatment of this disorder. The studies represent an extension of other studies in the field by now focusing on a newborn (as opposed to adult) model, by studying large animals (as opposed to rodents), and by performing long-term studies (weeks as opposed to days). We believe these features of this study will increase its translational potential. The major findings of these studies included the feasibility of scaffold implantation into direct continuity with native intestine, the development of a sustainable model for stoma maintenance in newborn piglets, and the development of a successful diverting ileostomy model in piglets. Furthermore, we describe a third surgical model in which we showed the feasibility of placing the scaffold directly into a blind loop of intestine, while restoring intestinal continuity. Taken together, these studies reveal the scope of three potentially useful approaches for the study of SBS and placement of an artificial intestine in the piglet.

It is noteworthy that these results leave room to address additional physiological responses induced by the individual models. Specifically, in some older swine, we found similar results to Agopian *et al.* with implanted scaffolds causing significant immune reaction and fibrosis,[34] yet this was not observed in the younger piglets. In addition, these studies provide some insights into the effects of age, innate variability

in the immune response, the local inflammatory response due to anastomosis of bare scaffold with native intestine, or bacterial contamination of the scaffold with gut flora that can be investigated further. We are particularly interested in whether bacterial overgrowth in bypassed loops could play a role in the success or failure of the graft.

The development of an experimental model to study the function of an artificial intestine also provides a platform in which to address several important yet unanswered questions in the field of tissue engineering. Specifically, does successful engraftment depend on the age of the donor and/or recipient animal? Could immunosuppression be necessary even when autotransplanting tissue to prevent the initial immune response? Is the omentum capable of generating vasculature complex enough to support full-sized intestinal constructs? Are there differences between fetal versus adult tissue sources, both with autotransplantation and allotransplantation? Would the administration of anti-inflammatory agents improve outcome of the implanted grafts? Questions such as these—which are important to answer if we are to ever bring an artificial intestine to clinical use—can now be investigated further using the large animal models presented in this study. Future studies will focus on the inflammatory response to the implanted grafts.

In conclusion, we have now described the development of three porcine surgical models to evaluate full segment constructs, two of which, to our knowledge, have not been previously described in large animals for this purpose. In addition, these models were employed to test tissue-engineered grafts in intestinal continuity over long time periods, on the order of 4–6 weeks. These studies provide a rationale for further assessment of the absorptive and mechanical properties of these implanted grafts, so as to enhance the development of an artificial intestine for the treatment of SBS.

Acknowledgments

M.R.L. received salary support during his contribution to this study under a National Institutes of Health National Institute of Diabetes and Digestive and Kidney Diseases T32 training grant (2T32DK007713-21). L.Y.M. received salary support during his contribution to this study under a National Institutes of Health National Institute of Diabetes and Digestive and Kidney Diseases T32 training grant (5T32DK007713-19).

Disclosure Statement

No competing financial interests exist.

References

1. Spencer, A.U., Neaga, A., West, B., *et al.* Pediatric short bowel syndrome: redefining predictors of success. Ann Surg **242,** 403, 2005.
2. Nucci, A., Cartland Burns, R., Armah, T., *et al.* Interdisciplinary management of pediatric intestinal failure: a 10-year review of rehabilitation and transplantation. J Gastrointest Surg **12,** 429, 2008.
3. Modi, B.P., Langer, M., Ching, Y.A., *et al.* Improved survival in a multidisciplinary short bowel syndrome program. J Pediatr Surg **43,** 20, 2008.
4. Fitzgibbons, S.C., Ching, Y., Yu, D., *et al.* Mortality of necrotizing enterocolitis expressed by birth weight categories. J Pediatr Surg **44,** 1072, 2009.
5. Diamond, I.R., de Silva, N., Pencharz, P.B., *et al.* Neonatal short bowel syndrome outcomes after the establishment of the first Canadian multidisciplinary intestinal rehabilitation program: preliminary experience. J Pediatr Surg **42,** 806, 2007.
6. Squires, R.H., Duggan, C., Teitelbaum, D.H., *et al.* Natural history of pediatric intestinal failure: initial report from the pediatric intestinal failure consortium. J Pediatr **4,** 723, 2012.
7. Wales, P.W. Surgical therapy for short bowel syndrome. Pediatr Surg Int **20,** 647, 2004.
8. Vacanti, J.P., Morse, M.A., Saltzman, W.M., Domb, A.J., Perez-Atayde, A., and Langer, R. Selective cell transplantation using bioabsorbable artificial polymers as matrices. J Pediatr Surg **23,** 3, 1988.
9. Grikscheit, T.C., Siddique, A., Ochoa, E.R., *et al.* Tissue-engineered small intestine improves recovery after massive small bowel resection. Ann Surg **240,** 748, 2004.
10. Levin, D.E., Barthel, E.R., Speer, A.L., *et al.* Human tissue-engineered small intestine forms from postnatal progenitor cells. J Pediatr Surg **48,** 129, 2013.
11. Sala, F.G., Matthews, J.A., Speer, A.L., Torashima, Y., Barthel, E.R., and Grikscheit, T.C. A multicellular approach forms a significant amount of tissue-engineered small intestine in the mouse. Tissue Eng A **17,** 1841, 2011.
12. Sala, F.G., Kunisaki, S.M., Ochoa, E.R., Vacanti, J., and Grikscheit, T.C. Tissue-engineered small intestine and stomach form from autologous tissue in a preclinical large animal model. J Surg Res **156,** 205, 2009.
13. Shaffiey, S.A., Jia, H., Keane, T., *et al.* Intestinal stem cell growth and differentiation on a tubular scaffold with evaluation in small and large animals. Regen Med **11,** 45, 2016.
14. Ladd, M.R., Niño, D.F., March, J.C., Sodhi, C.P., and Hackam, D.J. Generation of an artificial intestine for the management of short bowel syndrome. Curr Opin Organ Transplant **21,** 178, 2016.
15. Martin, L.Y., Ladd, M.R., Werts, A., Sodhi, C.P., March, J.C., and Hackam, D.J. Tissue engineering for the treatment of short bowel syndrome in children. Pediatr Res [Epub ahead of print]; DOI: 10.1038/pr.2017.234.
16. Workman, M.J., Mahe, M.M., Trisno, S., *et al.* Engineered human pluripotent-stem-cell-derived intestinal tissues with a functional enteric nervous system. Nat Med **23,** 49, 2017.
17. Kitano, K., Schwartz, D.M., Zhou, H., *et al.* Bioengineering of functional human induced pluripotent stem cell-derived intestinal grafts. Nat Commun **1,** 765, 2017.
18. Nakase, Y., Hagiwara, A., Nakamura, T., *et al.* Tissue engineering of small intestinal tissue using collagen sponge scaffolds seeded with smooth muscle cells. Tissue Eng **12,** 403, 2006.
19. Nakase, Y., Nakamura, T., Kin, S., *et al.* Endocrine cell and nerve regeneration in autologous in situ tissue-engineered small intestine. J Surg Res **137,** 61, 2007.
20. Costello, C.M., Sorna, R.M., Goh, Y., Cengic, I., Jain, N.K., and March, J.C. 3-D intestinal scaffolds for evaluating the therapeutic potential of probiotics. Mol Pharm **11,** 2030, **2014.**
21. Costello, C.M., Hongpeng, J., Shaffiey, S., *et al.* Synthetic small intestinal scaffolds for improved studies of intestinal differentiation. Biotechnol Bioeng **111,** 1222, 2014.
22. Costello, C.M., Phillipsen, M.B., Hartmanis, L.M., *et al.* Microscale bioreactors for in situ characterization of GI epithelial cell physiology. Sci Rep **7,** 12515, 2017.

23. Sung, J.H., Yu, J., Luo, D., Shuler, M.L., and March, J.C. Microscale 3-D hydrogel scaffold for biomimetic gastrointestinal (GI) tract model. Lab Chip **11,** 389, 2011.
24. Markowitz, J., Archibald, J., and Downie, H.G.. Intestinal fistulae: jejunostomy. In: Experimental Surgery Including Surgery. Physiology, 5th ed. Baltimore, MD: The Williams and Wilkins Company, 1964, pp. 143–163.
25. McCrackin, M.A., and Swindle, M.M. Gastrointestinal procedures. In: Swindle, M.M., and Smith, A.C., eds.. Swine in the Laboratory: Surgery, Anesthesia, Imaging and Experimental Techniques, 3rd ed. Boca Raton, FL: CRC Press, 2016, pp. 105–131.
26. Blikslager, A.T., Rhoads, J.M., Bristol, D.G., Roberts, M.C., and Argenzio, R.A. Glutamine and transforming growth factor-α stimulate extracellular regulated kinases and enhance recovery of villous surface area in porcine ischemic-injured intestine. Surgery **125,** 186, 1999.
27. Gonzalez, L.M., Moeser, A.J., and Blikslager, A.T. Porcine models of digestive disease: the future of large animal translational research. Transl Res **166,** 12, 2015.
28. Foell, D., Becker, F., Hadrian, R., Palmes, D., and Kebschull, L. A practical guide for small bowel transplantation in rats-review of techniques and models. J Surg Res **251,** 115, 2017.
29. Peck, B.C.E., Shanahan, M.T., Singh, A.P., and Sethupathy, P. Gut microbial influences on the mammalian intestinal stem cell niche. Stem Cells Int **1,** 5604727, 2017.
30. Yandza, T., Tauc, M., Saint-Paul, M.C., Ouaissi, M., Gugenheim, J., and Hébuterne, X. The pig as a preclinical model for intestinal ischemia-reperfusion and transplantation studies. J Surg Res **178,** 807, 2012.
31. Sato, T., Vries, R.G., Snippert, H.J., *et al.* Single Lgr5 stem cells build crypt-villus structures in vitro without a mesenchymal niche. Nature **459, 262, 2009.**
32. Fujii, M., Matano, M., Nanki, K., and Sato, T. Efficient genetic engineering of human intestinal organoids using electroporation. Nat Protoc **10,** 1474, 2015.
33. Loh, X.J., Karim, A.A., and Owh, C. Poly(glycerol sebacate) biomaterial: synthesis and biomedical applications. J Mater Chem B **39,** 7641, 2015.
34. Agopian, V.G., Chen, D.C., Avansino, J.R., and Stelzner, M. Intestinal stem cell organoid transplantation generates neomucosa in dogs. J Gastrointest Surg **13,** 971, 2009.

Address correspondence to:
David J. Hackam, MD, PhD
Bloomberg Children's Center
Division of Pediatric Surgery
Department of Surgery
Johns Hopkins University School of Medicine
Room 7323
1800 Orleans Street
Baltimore, MD 21287

E-mail: dhackam1@jhmi.edu

Received: February 2, 2018
Accepted: March 19, 2018
Online Publication Date: May 8, 2018